Journal of Alloys and Compounds 509 (2011) 6440–6446

Contents lists available at ScienceDirect

Journal of Alloys and Compounds

journal homepage: www.elsevier.com/locate/jallcom

Environmental friendly anodizing of AZ91D magnesium alloy in alkaline borate–benzoate electrolyte

Yan Liu[a,c], Zhongling Wei[b], Fuwei Yang[c], Zhao Zhang[a,d,*]

[a] Department of Chemistry, Zhejiang University, Hangzhou 310027, China
[b] Magnesium Technology Co., Ltd., Chinese Academy of Sciences, Jiaxing 314051, China
[c] Department of Chemistry, Tianshui Normal University, Tianshui 741000, China
[d] Key Laboratory for Light Alloy Materials Technology, Jiaxing 314051, China

ARTICLE INFO

Article history:
Received 1 September 2010
Received in revised form 11 March 2011
Accepted 15 March 2011
Available online 21 March 2011

Keywords:
Environmental friendly anodizing
Magnesium alloy
Sodium benzoate
Corrosion resistance

ABSTRACT

A kind of environmental friendly anodizing routine for AZ91D magnesium alloy, based on an alkaline borate–sodium benzoate electrolyte (NaBz) was studied. The effect of NaBz on the properties of the anodized film was investigated by scanning electron microscopy (SEM), X-ray diffraction (XRD), energy dispersive spectrometry (EDS), potentiodynamic polarization and electrochemical impedance spectroscopy (EIS), respectively. The results showed that the anodizing process, surface morphology, thickness, phase structure and corrosion resistance of the anodized film were strongly dependent on the concentration of NaBz. In the presence of adequate NaBz, a thick, compact and smoothing anodized film with excellent corrosion resistance was produced. Moreover, the forming mechanism of the anodized film in the presence of NaBz additive was also approached, which was a suppression of arc discharge process by the adsorption of Bz^- on the surface of magnesium alloy substrate.

1. Introduction

Magnesium alloys are widely used because of their excellent physical and mechanical properties such as low density and excellent mechanical strength [1]. However, the poor corrosion resistance of magnesium alloys hinders their further applications [2]. In marine climate, the magnesium alloy components for aircrafts and ships are unavoidably corroded by marine salts [3–5]. The rapid erosion of magnesium and its alloys in human body fluid or blood plasma often leads to the mechanical integrity loss of implant before the sufficient restoration of tissues [6].

To improve the corrosion resistance of magnesium and it alloys, various technologies such as alloying, surface modification, chemical conversion, electroplating, anodic oxidization, organic coatings, physical vapor deposition coating and plasma electrolytic oxidation (PEO) [7–9] have been developed. By contrast, more attentions and researches are expected to focus about the PEO technology because of the significant properties of the anodized film, such as good adhesion, high corrosion resistance and high hardness [10]. The anodized film with high hardness is excellent in tribological performance, which makes it an attractive material for automobile engine [11]. Besides, PEO technology is also widely used in aerospace, construction, electrical, biomedical, oil/gas processing, textile and sports and leisure sectors of industry [12].

However, environmental harmful inorganics (such as phosphate [13], fluoride [14] and aluminate [15] or toxic organics (such as hexamethylenetetramine [16] and 1H-benzotriazole [17]) are still employed in most of the existing PEO processes. In addition, the corrosion protection performance of the anodized films prepared by the existing methods is not adequate for the magnesium alloys in harsh service condition. Therefore, a simple and environmental friendly PEO process is needed to enhance the corrosion protection of magnesium and its alloys.

In this paper, an environmental friendly alkaline borate electrolyte using sodium benzoate (NaBz) as additive was studied for the PEO treatment of AZ91 magnesium alloy. NaBz is low-cost and intensively used in food [18], medicine [19] and corrosion protection of steel [20]. However, little has been done about the application research of NaBz in the corrosion protection of magnesium alloy. Compared with other additives used in the PEO process, such as phosphate [13], fluoride [14], aluminate [15], hexamethylenetetramine (LD 50 of 50 mg/kg, toxic) [16] and 1H-benzotriazole (LD 50 of 965 mg/kg, medium toxic) [17], NaBz (LD 50 of 4070 mg/kg, non-toxic) is safe and environmental friendly [21]. The effect of NaBz on the properties of the anodized films was investigated by scanning electron microscopy (SEM), X-ray diffraction (XRD), energy dispersive spectrometry (EDS), potentiodynamic

* Corresponding author. Tel.: +86 571 85615190.
E-mail address: eaglezzy@zjuem.zju.edu.cn (Z. Zhang).

0925-8388/$ – see front matter © 2011 Elsevier B.V. All rights reserved.
doi:10.1016/j.jallcom.2011.03.083

Table 1
Chemical composition of AZ91D magnesium alloy (wt%).

Al	Zn	Mn	Ni	Cu	Ca	Si	K	Fe	Mg
8.77	0.74	0.18	0.001	0.001	<0.01	<0.01	<0.01	<0.001	Balance

polarization and electrochemical impedance spectroscopy (EIS), respectively. Moreover, based on the results of the experiments, the forming mechanism of the anodized film in the presence of NaBz additive was also approached.

2. Experimental

2.1. Materials and specimen preparation

Prior to the PEO treatment, the AZ91D magnesium alloy (see Table 1) sheets with a size of 10 mm × 10 mm × 1 mm were polished up to 2000 grit, degreased with acetone, and washed with distilled water successively. The power supply was an AC power supply (110 V, 50 Hz) and the duration of the PEO process was 30 min. The basic anodic electrolyte was composed of 60 g/L NaOH, 25 g/L $Na_2B_4O_7$ and 20 g/L H_3BO_3. 0.0–3.0 g/L of NaBz (sodium benzoate: C_6H_5COONa) was used as additive. During the anodizing experiments, the temperature of the electrolyte was controlled at 30 °C by a miniature refrigerant equipment (model YT-8A, China).

Surface morphology of the anodized films was observed by a scanning electron microscopy (SEM, FEI SIRION-100). The chemical composition of the films was investigated with the energy dispersive X-ray spectroscopy (EDX) affiliated with SEM. The phase structure of the films was determined by X-ray diffractometry (XRD, AXS D8 ADVANCE), using Cu Kα (1.5418 Å) radiation source. The thickness of the films was measured using a Coating thickness Measurer (TT240, China). The program of Image J1.44e was used to calculate the surface porosity by treating the SEM photos of the anodized films [22]. The surface roughness (R_a) of the films was measured using a stylus type surface profilometer (E34-001) with accuracy of 0.01 μm. The density of the films was calculated from the weight gain and film thickness on a substrate with a fixed area (10 mm × 10 mm).

2.2. Electrochemical set up

To determine the corrosion resistance of the anodized films, potentiodynamic polarization and electrochemical impedance spectrum (EIS) were measured. Potentiodynamic polarization testing was carried out by a CHI 630D potentiostat (Chenhua, shanghai) at 25 ± 1 °C. Except the anodized film, the other part of the sample was coated with paraffin wax before any electrochemical testing. During the electrochemical test, the electric contacting was to the substrate material. A three electrode cell with the anodized film as working electrode, saturated calomel electrode as reference electrode and platinum sheet as counter electrode was employed in all the tests. The ratio of volume of neutral 3.5% NaCl solution (pH 7.03) to sample area was 50 mL/cm^2. After an initial delay of 15 min, scans were conducted at a rate of 1 mV/s from −0.25 V to 0.75 V (versus open circuit potential (OCP)). Electrochemical impedance spectrum (EIS) were measured using an impedance measurement unit (IM6e, Germany) over the frequency range of 0.01–10,000 Hz with a voltage amplitude of 5 mV in the neutral 3.5% NaCl solution.

3. Results and discussion

3.1. Anodized growth process

Fig. 1 shows the typical current density transient of the anodized process in the borate electrolyte containing 0–3.0 g/L of NaBz. Generally, the anodized growth process can be divided into two periods [23].

In the first period, the current density increases and reaches the maximum value rapidly. In the absence of NaBz, the current density changes acutely along with time. Violent sparking and gas release can be observed on the surface of the magnesium alloy specimen. However, in the presence of NaBz, the change of the current density becomes smaller and the intensity of the sparking and gas release is also reduced evidently. Nonetheless, when there is more than 2.0 g/L of NaBz in the electrolyte, further changes are not observed.

In the second period, the current density decreases gradually until a stabilized value is reached. The change of the current density is also strongly dependent on the concentration of NaBz. The current density decreases with the increasing of NaBz concentration. During this period, vigorous sparking and gas evolvement can still be observed in the absence of the NaBz. In the presence of NaBz, however, the sparking and gas evolvement are inhibited obviously.

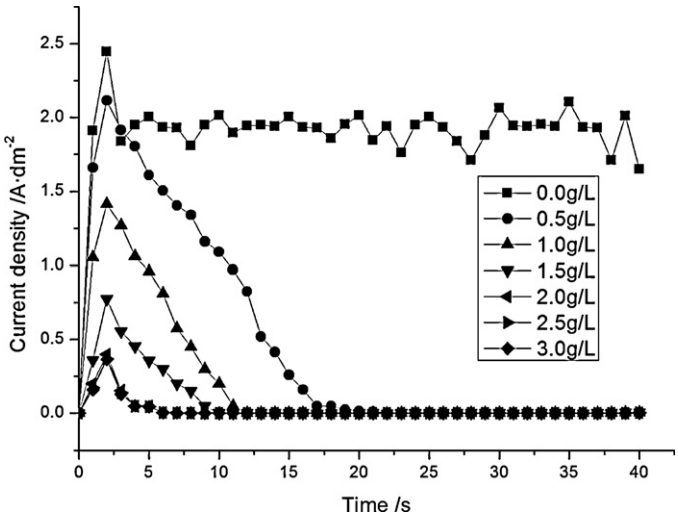

Fig. 1. Current density transient of the PEO process in the electrolyte with 0.0–3.0 g/L of NaBz.

Suitable anodizing current density is important for the PEO process. Vigorous sparking and gas evolvement at excessive high current density often result in poor anodized coating [24–27], while too low anodizing current density will make the formation of anodized films unachievable [28].

In this study, with the addition of NaBz in the electrolyte, the current density of PEO process is reduced and the vigorous sparking and gas evolvement are inhibited. Moderate PEO process at low current density facilitates the improvement of current efficiency [29] and the quality of anodized film [30].

3.2. Morphology and structure of anodized film

Fig. 2 presents the SEM images of the anodized films formed in the alkaline borate electrolyte with 0–3.0 g/L of NaBz. In the absence of NaBz, the anodized film (Fig. 2(a)) is relatively loose and coarse. There are many large-size of chunks, pores and high degree of cracks on the film. However, in the presence of NaBz, the large-size of chunks and pores decrease, the micro cracks disappear, and the anodized films become smoothing (Fig. 2(b)–(d), the concentration of NaBz is 1.0, 2.0 and 3.0 g/L, respectively). The surface porosity of the anodized films is presented in Fig. 3. With the increase of the concentration of NaBz, the large pores (>10.0 μm in size) and medium pores (5.0–10.0 μm in size) decrease rapidly. This suggests that these anodized films have more compact structure.

The roughness of the anodized films is listed in Fig. 4. With the increasing of the concentration of NaBz, the roughness of the anodized films decreases gradually. These results are consistent with the ones of SEM. The toughness of the anodized film is closely related with the anodizing current density in the PEO process [31]. In the absence of NaBz, the current density of the PEO process is very high. High current density often results in chunks, large size of pores and high degree of micro-cracks on the anodized film [28,33,34]. These chunks and large size of pores are responsible for the increased surface roughness [35]. In the presence of NaBz, the current density of the PEO process is reduced and the sparks become fine and moderate. Moderate PEO process is helpful for the formation of compact and smooth PEO film [36].

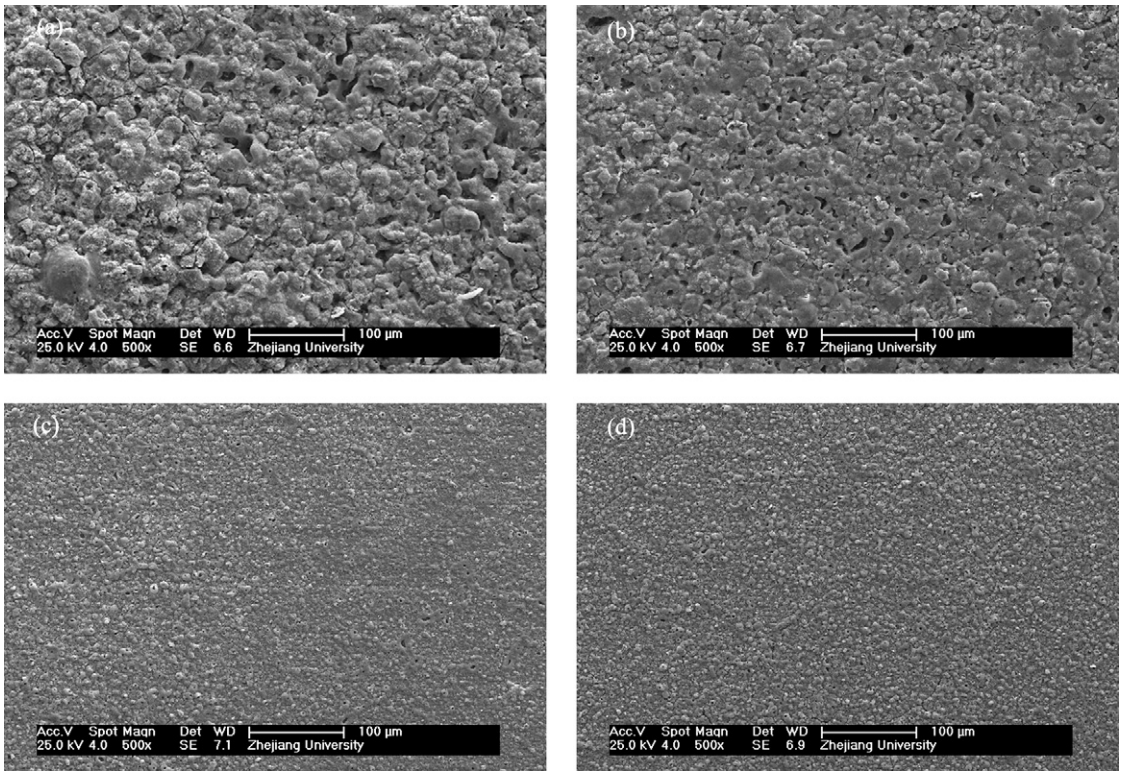

Fig. 2. SEM images of the anodized films formed in the electrolyte with (a) 0.0, (b) 1.0, (c) 2.0, (d) 3.0 g/L of NaBz.

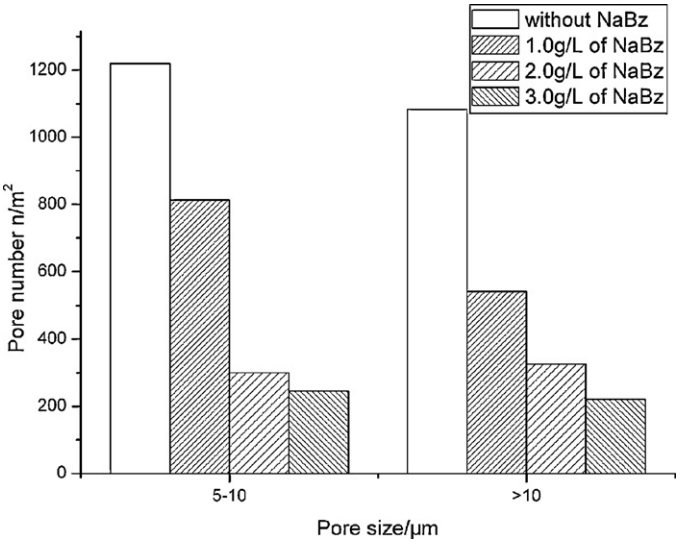

Fig. 3. Surface porosity of the anodized films formed in the electrolyte with 0–3.0 g/L of NaBz

The XRD results (Fig. 6) show that the anodized films consist mainly of MgO and Mg, as is in accordance with the results of the EDS. MgO is the results of the PEO process. The diffraction peaks of

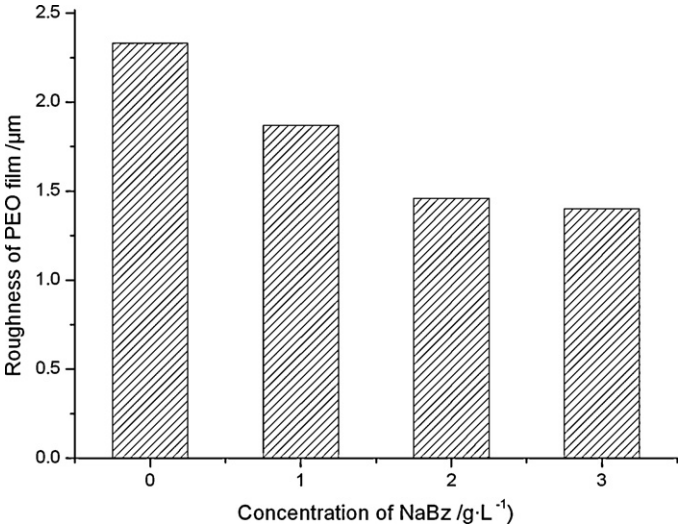

Fig. 4. Roughness of the anodized films formed in the electrolyte with 0–3.0 g/L of NaBz.

3.3. Phase structure analysis

EDS results of the anodized films are presented in Fig. 5 and Table 2. The results (Fig. 5(a) and (b)) show that the PEO films are mainly composed of O, Mg as well as a trace of Al and Na. Mg and Al come from the magnesium substrate. Na is from the electrolyte sodium hydroxide and NaBz. Element B is not detected. This suggests that B element has not been incorporated into the anodized films. In addition, the prepared anodized films in the presence of NaBz have more O, Al and less Mg (Table 2), as suggests a better corrosion resistance performance [37].

Table 2
EDS results of the anodized films formed in the electrolyte with 0.0–2.0 g/L of NaBz.

Concentration of NaBz (g/L)	Element weight (%)			
	O	Na	Mg	Al
0.0	35.80	1.58	56.53	6.09
1.0	35.84	1.55	55.52	6.40
2.0	35.87	1.63	55.51	6.99
3.0	35.89	1.68	55.49	7.02

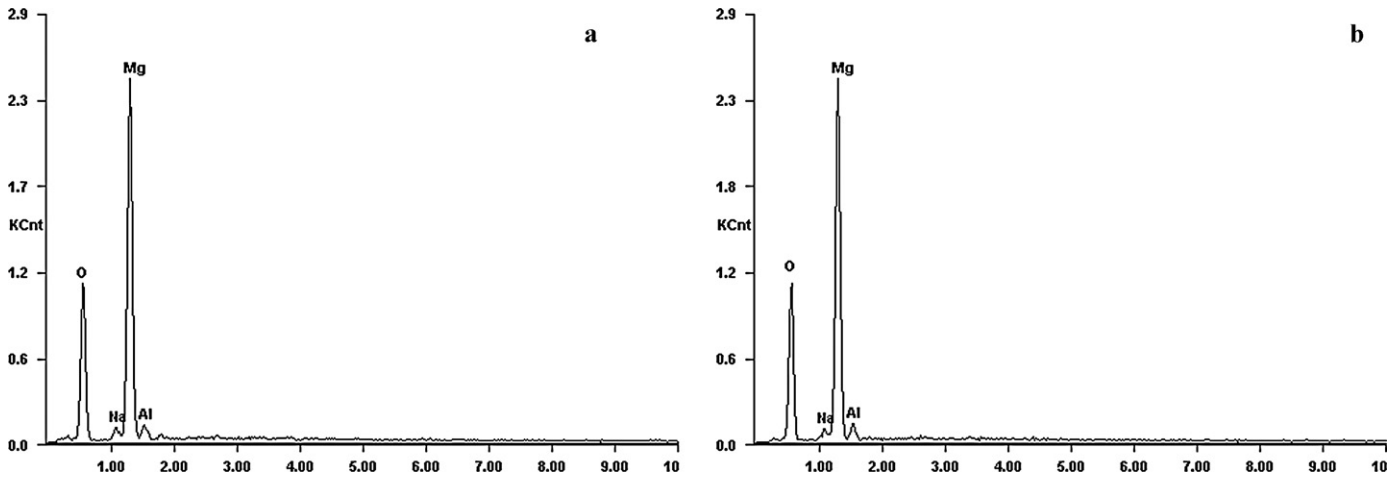

Fig. 5. EDS spectra of the anodized film formed in the electrolyte with (a) 0.0, (b) 2.0 g/L of NaBz.

Mg are from the magnesium alloy substrate. For the loose anodized film produced in the electrolyte without NaBz, X-ray can easily penetrate the film and detect the metal magnesium in the substrate. With the increasing of the NaBz concentration (0–2.0 g/L), the intensity of MgO peaks becomes stronger. The intensity of Mg peaks, however, decreases gradually and almost disappears when there is more than 2.0 g/L of NaBz in the electrolyte. These results are consistent with the results of SEM in Fig. 2.

3.4. Thickness test

The thickness evolution of the anodized films is listed in Table 3. In the absence of NaBz, the thickness of the anodized film is the biggest. In the presence of 0–2.0 g/L of NaBz, the thickness of anodized films reduces gradually. When there is more than 2.0 g/L of NaBz in the electrolyte, the thickness of the anodized films begins to stabilize. The thickness of the anodized film associates with the anodizing current density of the PEO process [38]. In the absence of NaBz additive, the anodizing current density of the PEO process is high. High current density can increase the growth rate and the thickness of the anodized film [39,40]. However, the anodized film formed at high current density is usually loose and porous [41–43]. Compared with the film formed at high current density, the anodized film formed at moderate current density is thinner, but it usually has more uniform and compact structure [44].

The density of the anodized films is listed in Table 3. In the electrolyte without NaBz, the prepared film has the lowest film density. The presence of NaBz, however, can increase the density of the film. When there is 2.0 g/L of NaBz in the electrolyte, the film density can increase 25.0%. The change of the film density is consistent with the results of the SEM in Fig. 2.

3.5. Corrosion resistance of the anodized film

The corrosion resistance of the anodized films was investigated by potentiodynamic polarization and electrochemical impedance.

The results of the potentiodynamic polarization are displayed in Fig. 7 and Table 4. Corrosion current density (j_{corr}), corrosion potential (E_{corr}) and polarization resistance (R_p) are used to evaluate the corrosion protective property of the anodized films. E_{corr} and j_{corr} can be obtained from the potentiodynamic polarization curves. R_p is calculated by the following relationship [45]:

$$R_p = \frac{\beta_a \beta_c}{2.303 j_{corr}(\beta_a + \beta_c)} \quad (1)$$

where β_a and β_c are anodic and cathodic tafel slope, respectively. For the anodized film formed in the absence of NaBz, E_{corr}, j_{corr}

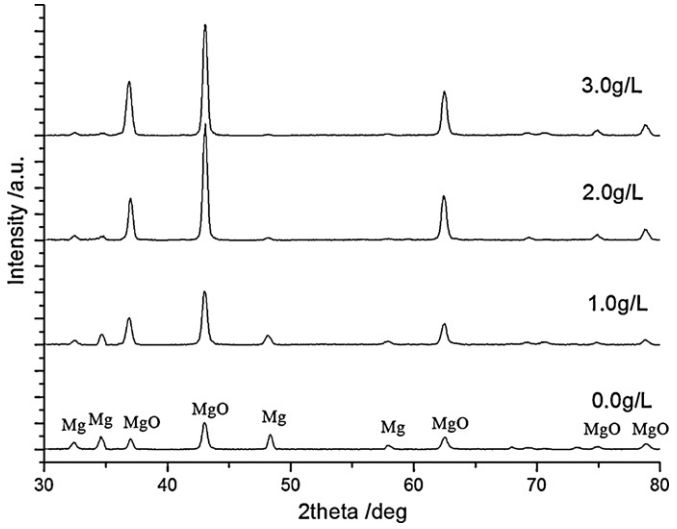

Fig. 6. XRD patterns of anodized films formed in the electrolyte with 0.0–3.0 g/L of NaBz.

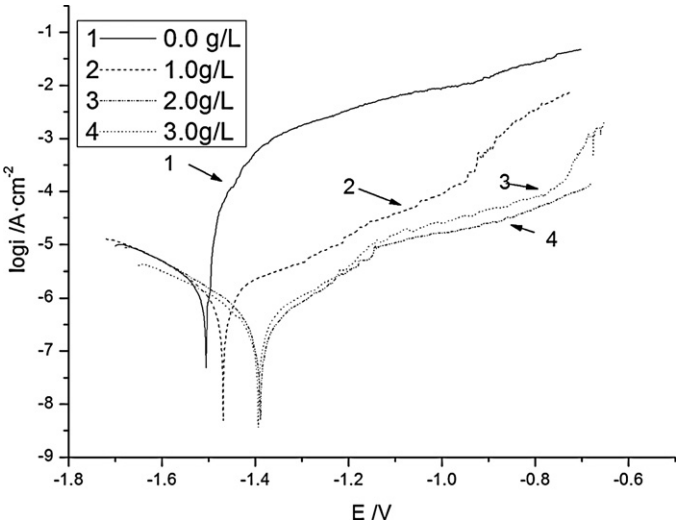

Fig. 7. Potentiodynamic polarization curves of anodized films formed in the electrolyte with 0.0–3.0 g/L of NaBz.

Table 3
Thickness of the anodized films formed in the electrolyte with 0.0–3.0 g/L of NaBz.

Concentration of NaBz (g/L)	0.0	0.5	1.0	1.5	2.0	2.5	3.0
Average thickness (μm)	39.18	32.23	28.45	26.35	22.23	22.25	22.28
Film density (g/cm^3)	1.40	1.56	1.68	1.72	1.75	1.76	1.76

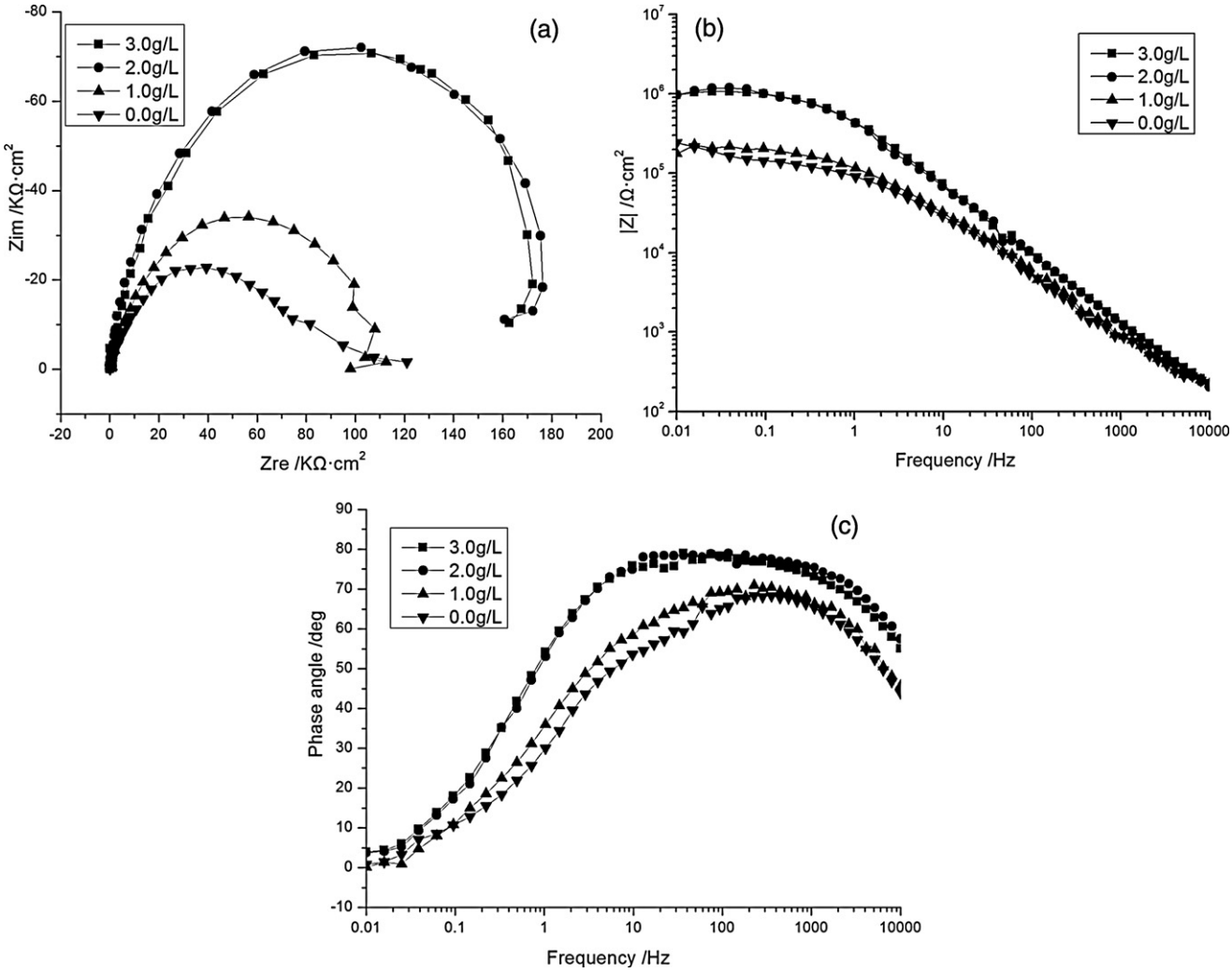

Fig. 8. EIS plots for the anodized films formed in the electrolyte with 0.0–3.0 g/L of NaBz.

and R_p are −1.502 V, 3.092×10^{-6} A/cm^2 and $3.532 \times 10^5\ \Omega\,cm^2$, respectively. For the anodized film formed in the electrolyte with NaBz, E_{corr} is shifted to the positive direction (Fig. 7), j_{corr} is reduced, and R_p is increased (Table 4). When there is 3.0 g/L of NaBz in the electrolyte, E_{corr}, j_{corr} and R_p are −1.389 V, 3.700×10^{-7} A/cm^2 and $3.369 \times 10^6\ \Omega\,cm^2$, respectively (Table 3). These results suggest a big enhance in the corrosion protection performance of the anodized films [17].

The results of the electrochemical impedance are displayed in Fig. 8. (a)–(c) are Nyquist diagrams, Z_{mod} Bode diagrams and phase angle Bode diagrams, respectively. As shown in Fig. 8(a), there are obvious low-frequency inductive loops for the anodized films produced in the electrolyte with 0.0–1.0 g/L of NaBz. This is caused by the pitting corrosion of the aggressive Cl^- in the electrolyte [46].

With the increasing of NaBz concentration, the diameter of the capacitive loop for the anodized films increases obviously (Fig. 8(a)), indicating a better anticorrosion performance. When the concentration of NaBz is more than 2.0 g/L, the diameter of the capacitive loop ceases to expand, suggesting the best anticorrosion performance has been achieved. Z_{mod} Bode diagrams in Fig. 8(b) can also be used to estimate the corrosion protection of the anodized films, and the results are in accordance with the ones of Nyquist diagrams.

For the anodized films formed in the solution containing 0.0–1.0 g/L of NaBz, a low frequency capacitive arc and a high frequency capacitive arc are observed in the phase angle Bode diagrams of Fig. 8(c). In general, the capacitive arcs of high and low

Table 4
Potentiodynamic polarization results for the anodized films formed in the electrolyte with 0.0–3.0 g/L of NaBz.

Concentration of NaBz (g/L)	E_{corr} (V)	β_a (mV)	β_c (mV)	R_p (Ω cm^2)	j_{corr} (A/cm^2)
0.0	−1.502	5.384	4.726	3.532×10^5	3.092×10^{-6}
1.0	−1.469	3.284	5.904	5.822×10^5	1.576×10^{-6}
2.0	−1.394	4.820	6.045	2.604×10^6	4.477×10^{-7}
3.0	−1.389	5.652	5.819	3.369×10^6	3.700×10^{-7}

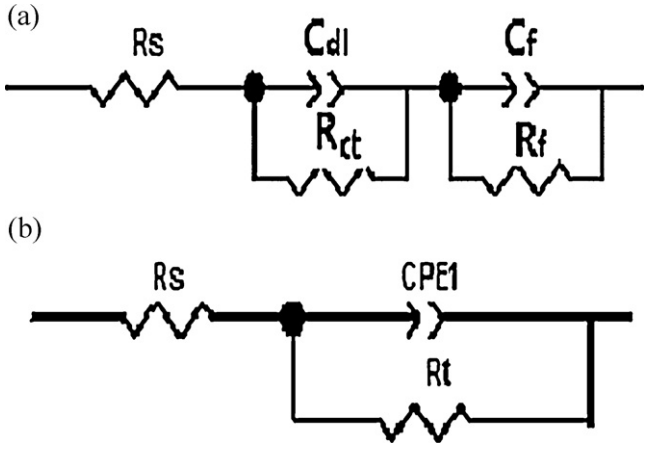

Fig. 9. Equivalent circuit for modeling the behavior of anodized films formed in the electrolyte with (a) 0.0–1.0, and (b) 2.0–3.0 g/L of NaBz.

Table 5
Typical impedance data of the anodized films formed in the electrolyte with 0.0–1.0 g/L of NaBz.

Concentration of NaBz (g/L)	R_s (Ω cm^2)	R_{ct} (Ω cm^2)	C_{dl} (μF/cm^2)	R_f (Ω cm^2)	C_f (μF/cm^2)
0.0	45.55	21424	0.92488	10132	1.5944
1.0	55.55	21718	0.57745	51445	1.0954

frequency domain represent the information of the outer and inner layers of the anodized film [47], respectively. The corrosion resistance of the anodized films can be also estimated quantitatively by simulating the experimental Bode diagrams using an equivalent circuit (Fig. 9(a)). The equivalent circuit is composed of two time constants in series with anodic film impedance and film/solution impedance. In this equivalent circuit, R_s represents the resistance of the solution, R_{ct} and C_{dl} are corresponding to the charge transfer resistance and the double layer capacitance respectively, C_f and R_f represent the capacitance and resistance of the anodized films. C_{dl} and C_f are dispersed capacity, which are caused by the irregular surface of the anodized films. The values of the fitting circuit elements are summarized in Table 5. It can be seen that the impedance of the spectrum are mainly determined by R_{ct} and R_f. Both of them increase with the increasing NaB_Z concentration. This is consistent with the results of R_p in Table 4.

In the presence of more than 1.0 g/L of NaBz, the prepared anodized films have only a high frequency capacitive arc and the low frequency capacitive arc is not detected. This indicates that these films have excellent corrosion resistance to NaCl solution. The improvement in corrosion resistance attributes to the compact structure and the good adhesion of the anodized films. As seen from the equivalent circuit in Fig. 9(b), the impedance measurement system consists of three parts: electrolyte, anodized film and metal/electrolyte interface. R_s is the resistance of the solution, CPE represents the double layer capacitance, and R_t is the charge transfer resistance of the anodic film. The impedance parameters are given in Table 6. The impedance of the spectrum is mainly depended on R_t. R_t increases with the increase of the NaBz concentration, as

Table 6
Typical impedance data of the anodized films formed in the electrolyte with 2.0–3.0 g/L of NaBz.

Concentration of NaBz (g/L)	R_s (Ω cm^2)	CPE-T (μF/cm^2)	CPE-P (n_t)	R_t (Ω cm^2)
2.0	47.28	0.17734	0.88239	97465
3.0	49.92	0.19595	0.86628	99316

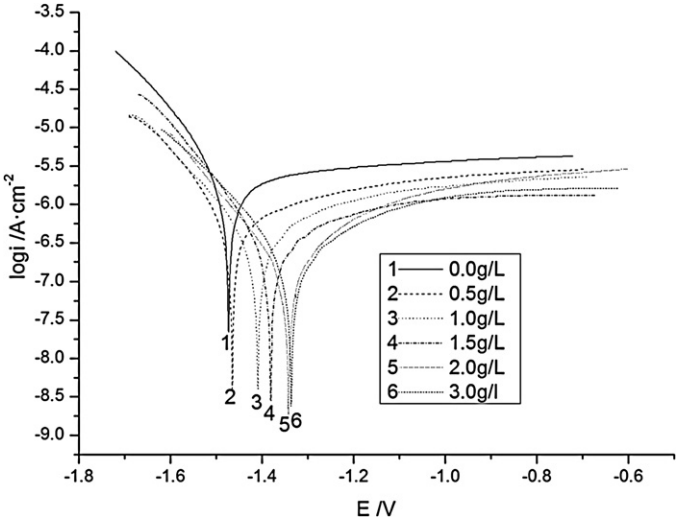

Fig. 10. Tafel curves of AZ91D magnesium alloy treated with 0.0–3.0 g/L of NaBz.

is same with the change of R_p in Table 4. The anodized films have the best corrosion resistance when the concentration of NaBz is more than 2.0 g/L. These results agree well with the ones of the potentiodynamic polarization.

3.6. Working mechanism of NaBz additive

The working mechanism of NaBz additive was studied and it was founded that it acted as an effective sparking inhibitor of the PEO process. As a kind of hard base, Bz^- can easily adsorb on the surface of magnesium alloy, where is rich in Mg^{2+} (hard acid) and form a monolayer adsorption on the surface of magnesium alloy [48]. The monolayer adsorption of Bz^- leads to the increase of surface resistance and the decrease of current density of the PEO process subsequently. This has been proved by our experimental results (Fig. 1). The Tafel curves of the magnesium alloy treated with 0–3.0 g/L of NaBz are displayed in Fig. 10. With the increase of the concentration of NaBz additive, the corrosion current density of magnesium alloy decreases and the corrosion potential increases, indicating the formation of Bz^- adsorption layer. The coverage rate (θ) of the surface of magnesium alloy by Bz^-, however, can be calculated from the corrosion current density of Tafel curves [49]:

$$\theta = 1 - \frac{j_{corr}}{j_{corr,o}} \quad (2)$$

where j_{corr} and $j_{corr,o}$ are the corrosion current density in the presence and absence of NaBz, respectively. The θ obtained is listed in Table 7. In the concentration range of 0–2.0 g/L, θ rises sharply and thereafter reaches a steady value when the concentration of NaBz exceeds 2.0 g/L. This is consistent with the change of current density (Fig. 1). These results indicate that the reduction of current density in the PEO process is the sequence of the addition of NaBz. Thus, the current density of PEO process can be controlled

Table 7
Surface coverage rate of the AZ91D magnesium alloy treated with 0.0–3.0 g/L of NaBz.

Concentration of the NaBz (g/L)	j_{corr} (A/cm^2)	E_{corr} (V)	θ (%)
0.0	1.771×10^{-6}	−1.563	0.00
0.5	6.038×10^{-7}	−1.465	65.91
1.0	3.285×10^{-7}	−1.409	81.45
1.5	2.523×10^{-7}	−1.401	85.75
2.0	1.407×10^{-7}	−1.343	92.02
3.0	1.401×10^{-7}	−1.337	92.09

by the addition of NaBz in the electrolyte. Generally, furious sparking at high current density result in large size of chunks, pores and higher degree of micro-cracks on the anodized film [50]. This kind of anodized film is poor in quality. Moderate sparking at low current density, however, can eliminate pit ablation and facilitate the formation of high quality anodized coating [51]. In fact, in the presence of 2.0 g/L of NaBz, a smooth, compact and ivory-white film can be produced (Fig. 2(c)). This kind of anodized film with good adhesion to substrate has excellent corrosion resistance (Figs. 7 and 8 and Table 4).

4. Conclusions

1. The PEO treatment of AZ91 magnesium alloy in the alkaline borate electrolyte was investigated. It was found that the PEO process was strongly dependent on the concentration of the additive NaBz. In the presence of NaBz, violent sparking and gas release were restrained, and a moderate PEO condition was obtained.
2. In the presence of NaBz, the quality of the anodized film was greatly improved. The size of the pores was reduced, the micro-cracks on the anodized film were eliminated, and an anodized film with compact structure and smoothing appearance was produced. Electrochemical testing results showed the anodized film obtained was excellent in corrosion resistance.
3. The working mechanism of NaBz additive was studied. Bz^- could adsorb on the surface of magnesium alloy and form a monolayer adsorption. Owing to the formation of absorption layer, the electric resistance of the magnesium alloy was increased, and the current density of the PEO process was decreased subsequently. In the presence of adequate NaBz additive, a moderate and controllable PEO process was founded, which facilitated the formation of high quality anodized film.

Acknowledgements

This work was supported by the National Natural Science Foundation of China (Project 50771092, 21073162), the Science and Technology Commission of Shanghai Municipality (Project 08JC1421600) and the Science and Technology Bureau of Jiaxing Municipality (Project 2008AZ2018).

References

[1] J.Q. Wang, Z.L. Ding, F.J. Qi, H. Zhu, Y.C. Fan, J. Alloys Compd. 24 (2010) 322–325.
[2] L. Wang, T. Shinohar, B.P. Zhang, J. Alloys Compd. 496 (2010) 500–507.
[3] M.C. Merino, A. Pardo, R. Arrabal, S. Merinob, P. Casajús, M. Mohedano, Corros. Sci. 52 (2010) 1696–1704.
[4] M. Jönsson, D. Persson, C. Leygraf, Corros. Sci. 50 (2008) 1406–1413.
[5] E. Huttunen-Saarivirta, V.-T. Kuokkala, J. Kokkonen, H. Paajanen, Mater. Chem. Phys. 126 (2011) 138–151.
[6] N.T. Kirkland, J. Lespagnol, N. Birbilis, M.P. Staiger, Corros. Sci. 52 (2010) 287–291.
[7] S. Candan, M. Unal, E. Koc, Y. Turen, E. Candan, J. Alloys Compd. 509 (2011) 1958–1963.
[8] R. Pinto, M.J. Carmezima, M.G.S. Ferreira, M.F. Montemor, Electrochim. Acta 55 (2010) 2482–2489.
[9] M. Carboneras, L.S. Hernández, J.A. del Valle, M.C. García-Alonso, M.L. Escudero, J. Alloys Compd. 496 (2010) 442–448.
[10] M. Laleh, A.S. Rouhaghdam, T. Shahrabi, A. Shanghi, J. Alloys Compd. 496 (2010) 548–552.
[11] J. Guo, L.P. Wang, J. Liang, Q.J. Xue, F.G. Yan, J. Alloys Compd. 48 (2009) 903–909.
[12] F.C. Walsh, C.T.J. Low, R.J.K. Wood, K.T. Stevens, J. Archer, A.R. Poeton, A. Ryder, Trans. Inst. Met. Finish. 87 (2009) 122–135.
[13] L. Wang, L. Chen, Z.C. Yan, H.L. Wang, J.Z. Peng, J. Alloys Compd. 493 (2010) 445–452.
[14] G.H. Lv, H. Chen, X.Q. Wang, H. Pang, G.L. Zhang, B. Zou, H.J. Leed, S.Z. Yang, Surf. Coat. Technol. 205 (2010) 36–40.
[15] P.S. Santosh, A. Yoshitaka, H. Hiroki, Mater. Trans. 51 (2010) 99–102.
[16] A. Bai, Z.J. Chen, Surf. Coat. Technol. 203 (2009) 1956–1963.
[17] X.H. Guo, M.Z. An, P.X. Yang, H.X. Li, C.N. Su, J. Alloys Compd. 482 (2009) 487–497.
[18] A. Bevilacqua, M.R. Corbo, M. Sinigaglia, Food Bioprocess Technol. 4 (2010) 1–7.
[19] J. Breitkreutz, M. Bornhöft, F. Wöll, P. Kleinebudde, Eur. J. Pharm. Biopharm. 56 (2003) 247–253.
[20] V. Afshari, C. Dehghanian, J. Solid State Electrochem. 14 (2010) 1855–1861.
[21] Acute toxicity test (GB 15193.3-2003).
[22] R. Ziel, A. Haus, A. Tulke, J. Membr. Sci. 323 (2008) 241–246.
[23] G.H. Lv, H. Chen, W.C. Gu, L. Li, E.W. Niu, X.H. Zhang, S.Z. Yang, J. Mater. Process. Technol. 208 (2008) 9–13.
[24] C.S. Wu, Z. Zhang, F.H. Cao, J.Q. Zhang, C.N. Cao, Appl. Surf. Sci. 253 (2007) 3893–3898.
[25] C.E. Barchiche, E. Rocca, C. Juers, J. Hazan, J. Steinmetz, Electrochim. Acta 53 (2007) 417–425.
[26] M.J. Li, T. Tamura, N. Omura, K. Miwa, J. Alloys Compd. 487 (2009) 187–193.
[27] V. Raj, M. Mubarak Ali, J. Mater. Process. Technol. 209 (2009) 5341–5352.
[28] O. Khaselev, D. Weiss, J. Yahalom, Corros. Sci. 43 (2001) 1295–1307.
[29] E. Matykina, R. Arrabal, P. Skeldon, G.E. Thompson, Surf. Interface Anal. 42 (2010) 221–226.
[30] H.L. Wu, Y.L. Cheng, L.L. Li, Z.H. Chen, H.M. Wang, Z. Zhang, Appl. Surf. Sci. 253 (2004) 9387–9394.
[31] J. Liang, L.T. Hu, J.C. Hao, Appl. Surf. Sci. 253 (2007) 6939–6945.
[33] H.F. Guo, M.Z. An, S. Xu, H.B. Huo, Thin Solid Films 485 (2005) 53–58.
[34] Y.H. Wang, J. Wang, J.B. Zhang, Z. Zhang, Matter. Lett. 60 (2006) 474–478.
[35] Y.K. Lee, K.S. Lee, T. Jung, Electrochem. Commun. 10 (2008) 1716–1719.
[36] L.Y. Chai, X. Yu, Z.H. Yang, Y.Y. Wang, M. Okido, Corros. Sci. 50 (2008) 3274–3279.
[37] F.H. Cao, Z. Zhang, J.Q. Zhang, C.N. Cao, Mater. Corros. 58 (2007) 696–703.
[38] Y.J. Zhang, C.W. Yan, F.H. Wang, H.Y. Lou, C.N. Cao, Surf. Coat. Technol. 161 (2002) 36–43.
[39] Z.P. Yao, Y.J. Xu, Z.H. Jiang, F.P. Wang, J. Alloys Compd. 488 (2009) 273–278.
[40] R.H.U. Khan, A. Yerokhin, X. Li, H. Dong, A. Matthews, Surf. Coat. Technol. 205 (2010) 1679–1688.
[41] S. Verdier, M. Boinet, S. Maximovitch, F. Dalard, Corros. Sci. 47 (2005) 1429–1444.
[42] H.M. Wang, Z.H. Chen, L.L. Li, Surf. Eng. 26 (2010) 385–391.
[43] Y. Chen, X. Nie, D.O. Northwood, Surf. Coat. Technol. 205 (2010) 1774–1782.
[44] Z. Shi, G. Song, A. Atrens, Corros. Sci. 48 (2006) 1939–1953.
[45] M.G. Fontana, Corrosion Engineering, 3rd ed., Mc Graw-Hill International Editions, 1996, p. 42.
[46] L. Wang, L. Chen, Z.C. Yan, H.L. Wang, J.Z. Peng, J. Alloys Compd. 480 (2009) 469–474.
[47] S.J. Xia, R. Yue, R.G. Rateick, V.I. Briss, J. Electrochem. Soc. 151 (2004) B179–B187.
[48] M. Hojo, T. Ueda, M. Ike, M. Kobayashi, H. Nakai, J. Mol. Liq. 145 (2009) 152–157.
[49] G. Blustein, R. Romagnoli, J.A. Jáen, A.R. Di Sarli, B. del Amo, Colloids Surf. A 290 (2006) 7–18.
[50] R.F. Zhang, D.Y. Shan, R.S. Chen, E.H. Han, Mater. Chem. Phys. 107 (2008) 356–363.
[51] R.O. Hussein, X. Nie, D.O. Northwood, Surf. Coat. Technol. 205 (2010) 1659–1667.